THE JOURNAL OF PHYSICAL CHEMISTRY A

Article

pubs.acs.org/JPCA

Prediction of Thymine Dimer Repair by Electron Transfer from Photoexcited 8-Aminoguanine or Its Deprotonated Anion

Iwona Sieradzan,[†] Marzena Marchaj,[†] Iwona Anusiewicz,[†] Piotr Skurski,[†,‡] and Jack Simons*[,‡]

[†]Department of Chemistry, University of Gdańsk, Wita Stwosza 63, 80-308 Gdańsk, Poland

[‡]Chemistry Department and Henry Eyring Center for Theoretical Chemistry, University of Utah, Salt Lake City, Utah 84112, United States.

ABSTRACT: Electronic structure methods are used to estimate *differences* in reaction barriers for transfer of an electron from singlet $\pi\pi^*$ excited 8-aminoguanine (A) or deprotonated 8-aminoguanine anion (A^-) to a proximal thymine dimer site compared to barriers when $\pi\pi^*$ excited 8-oxoguanine (O) or deprotonated 8-oxoguanine (O^-) serve as the electron donor. It is predicted that the barrier for photoexcited A should be lower than for photoexcited O, and the barrier for photoexcited A^- should be lower than for photoexcited O^-. Moreover, A, O^-, and A^- are predicted to have $\pi\pi^*$ excited states at energies near where O does, which allows them to be excited by photons low enough in energy to avoid exciting or ionizing any of DNA's bases. The origin of the differences in barriers is suggested to be the lower ionization potential of A compared to O and the lower electron detachment energy of A^- compared to O^-. Because O and O^- have been experimentally shown to produce thymine dimer repair, it is proposed that A and A^- are promising repair agents deserving experimental study.

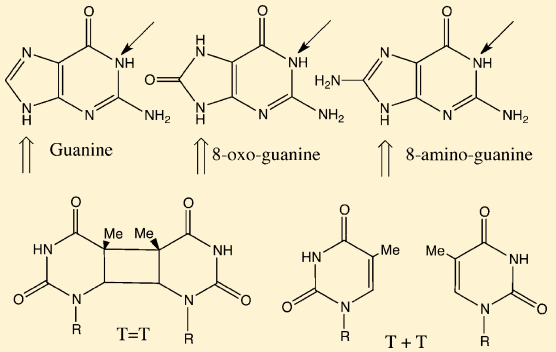

1. INTRODUCTION

In two recent papers,[1,2] we offered qualitative theoretical interpretations of earlier experimental data[3,4] relating to the rate of thymine dimer repair induced by $\pi\pi^*$ photoexcitation of 8-oxoguanine (O) derivatives proximal to the thymine dimer. The O molecules are especially attractive as repair agents because they absorb light at energies below where the thymine dimer or any of DNA's bases have $\pi\pi^*$ absorptions (so they can be selectively excited) and because they have ionization potentials (IP) lower than any DNA base (which makes them excellent candidates for electron donation to the thymine dimer site). In the present paper, we report results and predictions for an alternative repair agent, 8-aminoguanine (A), whose study was suggested to us by Prof. C. J. Burrows and members of her group. The A species is found to have a singlet $\pi\pi^*$ excited state close to that of O (and outside the range of DNA's bases' $\pi\pi^*$ absorptions) and to have an even lower IP than O, thus motivating us to undertake this study.

Thymine dimers (T=T) can be formed in DNA by exposure to ultraviolet light that excites a $\pi\pi^*$ transition within the thymine monomer, which then renders feasible the [2+2] cyclo-addition ring-forming reaction linking the two thymines. Because thymine dimers pose a danger as an initial stage in certain skin cancers, it is of much interest to identify and characterize small molecules that can repair T=T damage by converting T=T into two intact thymines (T + T). In Figure 1 we show the structures of guanine, O, A, and T=T and of the two separated units into which T=T is cleaved when the damage is repaired.

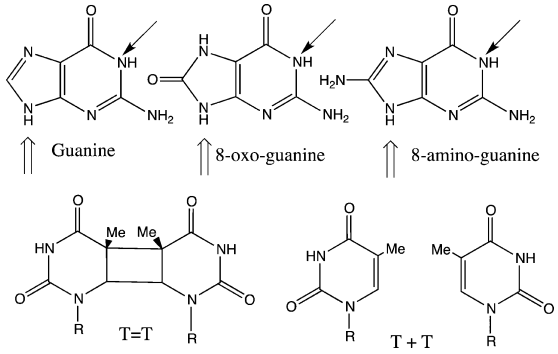

Figure 1. Molecular structures of guanine, 8-oxoguanine, and 8-aminoguanine and of the thymine dimer (in cis-syn geometry) and two separated thymine units. Also shown by the upper arrows are the sites of deprotonation when the anions studied here are produced. The lower arrows and the symbols R show the sites at which these species are bound to sugar units when they occur within a DNA strand.

As explained in refs 1 and 2, the repair process is believed to involve (i) initial photoexcitation of the electron donor, followed by (ii) electron transfer from the excited donor to the T=T acceptor taking place in competition with radiationless and radiative decay of the excited donor, followed by (iii) rapid

Special Issue: Kenneth D. Jordan Festschrift

Received: August 1, 2013
Revised: December 23, 2013
Published: January 2, 2014

bond cleavages within the T=T$^-$ anion to form T + T$^-$, and then (iv) by return of the electron from T$^-$ to the donor cation. As also explained in refs 1 and 2, the electron transfer is thought to be the rate-limiting step.

As detailed in ref 2, it is believed that photoexcited O decays back to the ground electronic state within ca. 10−100 ps (the latter value applies when the O is excited near the origin of its $\pi\pi^*$ band; the former applies when the $\pi\pi^*$ excited O is produced with excess vibrational energy that allows the system to better access conical intersections that return it to the ground state). On the basis of the 1% quantum yield for T=T repair by O determined in ref 4, this means the electron-transfer rate and thus of T=T repair is ca. 10^8−10^9 s^{-1}. Because the experiments of refs 3 and 4 were carried out at 22°C, we can say that the barrier for electron transfer cannot exceed ca. 0.23 eV to achieve rates of 10^8 s^{-1}, respectively, because the barrier-access rate can be no less than the rate of electron transfer.

In ref 3, DNA duplexes such as shown in Figure 2 were exposed at 22 °C to ultraviolet radiation filtered to exclude

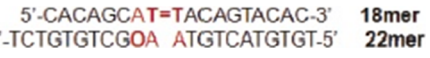

Figure 2. Example of the DNA duplexes containing a thymine dimer (T=T) and an 8-oxoguanine (O) unit. Taken from ref 1

photons having energy in excess of 4.1 eV. By using photons below 4.1 eV, the workers of ref 3 could be assured that only the O moiety was being electronically excited; neither T=T nor any of the DNA bases absorb below 4.1 eV. After irradiation for a length of time *t*, the sample was subjected to chromatographic analysis to determine what fraction of the thymine dimers had been converted to two intact thymine units. Such experiments were carried out with the O unit inserted in various locations (e.g., on the same strand at the T=T or on the opposite strand; to the 5′ or 3′ side of the T=T; and at various distances from the T=T), and the yield of T=T conversion to T + T was determined for each such position of the O.

The fraction of T=T repair was found to vary with placement of the O unit relative to the T=T in a manner that we rationalized in ref 1 in terms of variations in the efficiency of electron transfer from the photoexcited O to the T=T to generate a T=T$^-$ anion.

There were two interesting features of how the T=T repair yields of ref 3 varied that were addressed in ref 1. First, no detectable repair was observed when the O and T=T sites were separated by ca. 10 Å (measured as the distance *R* between the midpoint of T=T's cyclobutane ring and the center of O's six-membered ring), a distance near that of the third nearest neighbors. Second, the repair yields appeared to vary with *R* as $\exp(-\beta R)$ with β ca. 0.6 Å^{-1} for distances ranging between ca. 3.5 Å and ca. 7 Å, which are distances characteristic of nearest to second nearest neighbors. The former observation was proposed[1] to result because the Coulomb interaction energy between the O$^+$ donor cation and T=T$^-$ acceptor anion is sufficiently stabilizing to make the energy barrier thermally accessible only for *R* values less than ca. 10 Å.

In ref 4, solution-phase experiments similar to those reported in ref 3 were carried out, but with the O and T=T units attached to solubilizing groups at the locations labeled with the lower arrow or by *R* in Figure 1, respectively. That is, the O and T=T were not bound within DNA strands but dissolved in solutions containing 0.2 mM O and 0.2 mM T=T. These solutions were exposed to the same filtered ultraviolet light described above for a length of time *t*, and the fraction of T=T repair was determined. In addition, in ref 4, these same experiments were performed at solution pH values above the pK_a = 8.6 of O, where the O molecule is expected to be deprotonated at the position labeled by the top arrow in Figure 1 and thus to exist as an anion that we denote O$^-$. Under such high-pH conditions, the rate of T=T repair was found to increase by a factor of ca. 10 compared to the rate at pH values where O is not deprotonated, so it was concluded that O$^-$ is a better repair agent than O.

In ref 2 we were able to rationalize the ca. 10-fold increase in the rate of T=T repair observed under pH conditions where the O is expected to be deprotonated. To do so, we analyzed the energetics of the electron-transfer process in which a photoexcited O$^-$ anion is the electron donor. The fact that it costs less energy to detach an electron from the O$^-$ anion than from neutral (not deprotonated) O was suggested[2] to cause the 10-fold increase in the T=T repair rate when O$^-$ is used as the electron donor.

In the present paper, we employ methods similar to those used in refs 1 and 2 to compare the electron-transfer barriers when O is used as the electron donor to those when 8-aminoguanine is used as the donor. We also consider the case in which deprotonated 8-aminoguanine is used as the donor. Although there are uncertainties in the electronic structure-based free energies we compute, we think the *differences* in computed ionization potentials, electron detachment energies, and solvent reorganization energies among the four donor species are reliable enough to allow us to identify key differences among A, O, A$^-$, and O$^-$ as electron donors and to suggest which is likely to yield the highest T=T repair rates. It is the similarity in geometries and π-orbital structures of A and O (and of A$^-$ and O$^-$) that cause us to posit that our computational approach can produce reliable predictions for *differences* between A and O and between A$^-$ and O$^-$.

In section 2, we detail the computational methods employed, section 3 gives our results, and section 4 provides an overview and conclusions. Before describing the kind of electronic structure calculations we carried out, it is useful to review how the data thus obtained are used to determine the parameters of Marcus theory,[5] which ultimately allows us to estimate the relative energy barriers for T=T repair. In Figure 3, we display three parabolas that describe how the energies of three

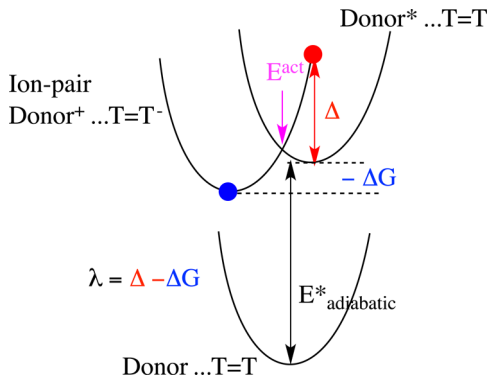

Figure 3. Parabolas relating to the ground-state donor···T=T (lower), photoexcited donor*···T=T (upper right) and charge-transferred donor $^+$···T=T$^-$ (upper left) states. The meanings of the symbols shown in the figure are given in the text.

dx.doi.org/10.1021/jp411666a | J. Phys. Chem. A 2014, 118, 7194−7200

electronic states vary as functions of a coordinate that characterizes the solvent's low-frequency dielectric response and the donor A and T=T molecules' geometrical relaxation. The three states are (i) the ground electronic state of the A···T=T pair, (ii) the photoexcited state of this same pair (which is the state from which the electron transfer begins), and (iii) the ion-pair state $A^+\cdots T{=}T^-$ produced upon electron transfer (which is the state formed upon electron transfer).

In Figure 3, ΔG is the Gibbs free energy change (shown as negative here) associated with transfer of an electron from donor* to T=T allowing the geometries of donor* and T=T to relax to those appropriate to the donor$^+$ cation and T=T$^-$ anion and allowing for the solvent to fully relax (i.e., allowing for its static dielectric response). Also in Figure 3, Δ is the Gibbs free energy change associated with transfer of an electron from donor* to T=T, keeping the geometries of donor* and T=T frozen (at their respective equilibrium values as determined in geometry optimization under equilibrium solvation) and allowing the solvent to respond only via its high-frequency dielectric constant (i.e., allowing for nonequilibrium response to the electron transfer). $E^*_{\text{adiabatic}}$ is the adiabatic electronic excitation energy of the donor; that is, the energy of the $\pi\pi^*$ excited donor* at its equilibrium (in water) geometry minus the energy of the ground-state donor at its own equilibrium geometry. Finally, the reorganization energy is $\lambda = \Delta - \Delta G$, and the Marcus activation energy is calculated as $E^{\text{act}} = (\lambda + \Delta G)^2/4\lambda$. In section 2, we detail how these parameters are computed using conventional electronic structure theory.

2. METHODS

The equilibrium geometries and free energies of the deprotonated anionic A$^-$ and O$^-$ and the nondeprotonated neutral A and O donors were determined at the second-order Møller–Plesset (MP2) perturbation level with 6-31++G(d,p)[6,7] basis sets as were the structures and free energies of the radical neutrals A$^\bullet$ and O$^\bullet$ formed by detaching an electron from A$^-$ and O$^-$ and the radical cations A$^+$ and O$^+$ formed by removing an electron from A and O. The free energies and structures for T=T and T=T$^-$ were determined by using similar methods (the basis set was augmented with additional diffuse functions as described in ref 1). All of these geometry optimizations and MP2 energy determinations were carried out in the presence of water solvation modeled as discussed below. In addition, these geometry optimization steps were repeated within the DFT framework using Becke's three-parameter hybrid method with the LYP (Lee–Yang–Parr) correlation functional (B3LYP).[8,9]

To approximate the effect of surrounding solvent molecules on the electronic energies, we employed the polarized continuum (PCM) solvation model[10−12] within a self-consistent reaction field treatment, as implemented in the Gaussian09 program. From these calculations, free energies for the neutral, cation, and anion species are obtained that contain enthalpic and entropic contributions from the solute and solvent. Hence, the anion electron detachment energy (DE), neutral electron affinity (EA), neutral ionization potential (IP), and $\pi\pi^*$ excitation energy data we report later reflect these solvent thermodynamic effects and thus are free energies.

The singlet $\pi\pi^*$ electronic excitation energies of A, O, A$^-$, and O$^-$ were obtained from the TD-DFT[13−15] technique using Becke's three-parameter hybrid method with the LYP (Lee–Yang–Parr) correlation functional (B3LYP)[8,9] and 6-31++G(d,p) basis set. These excitation energies were obtained both at the equilibrium geometry of the absorbing species including only nonequilibrium solvent response (i.e., as vertical quantities) and by allowing for both geometry relaxation and equilibrium solvent response upon excitation (i.e., as adiabatic quantities which we report as $E^*_{\text{adiabatic}}$). The geometry optimizations of the $\pi\pi^*$ excited states were performed at the TD-DFT level and within MP2 theory (in the MP2 case, optimization was performed on the triplet $\pi\pi^*$ state, but triplet energies were not used to determine the Δ and ΔG parameters; only DFT energies at MP2 geometries were used).

In addition, vertical TD-DFT excitation energies belonging to the charge-transfer state of O···T=T complexes were computed at various O-to-T=T distances employing the long-range-corrected version of B3LYP using the Coulomb-attenuating method denoted CAM-B3LYP.[16] This study was carried out to test whether our approach for determining Δ and ΔG in terms of donor IPs (or DEs) and T=T EAs plus Coulomb interactions would yield results of accuracy equal to those obtained by direct TD-DFT calculation on the donor–acceptor complex. These calculations were especially challenging because we had to compute many excited electronic states and inspect their orbital occupancies to identify the desired charge-transfer state. All of the calculations were performed with the Gaussian09 program.[17]

To determine all of the energy parameters needed to employ Marcus theory in estimating the electron-transfer rates, we carried out several series of MP2- and DFT-level calculations as we now describe for the neutral A donor and the T=T acceptor.

1. We computed the energy $E_A(A)$ of neutral A at its equilibrium geometry in a dielectric environment having $\varepsilon = 78$ (because the experiments we hope to influence are carried out in aqueous solution) allowing for full equilibrium solvation.
2. We computed the energy $E_{A^+}(A^+)$ of the cation A$^+$ at its equilibrium geometry in a dielectric environment having $\varepsilon = 78$ again allowing for full equilibrium solvation. $E_{A^+}(A^+) - E_A(A)$ gives the adiabatic IP of A, $\text{IP}_{\text{adiabatic}}(A)$.
3. We computed the energy $E_{TT}(TT)$ of neutral T=T at its equilibrium geometry in a dielectric environment having $\varepsilon = 78$ allowing for full equilibrium solvation.
4. We computed the energy $E_{TT-}(TT^-)$ of anionic T=T$^-$ at its equilibrium geometry in a dielectric environment having $\varepsilon = 78$ allowing for full equilibrium solvation. $E_{TT}(TT) - E_{TT-}(TT^-)$ gives the adiabatic EA of T=T, $\text{EA}_{\text{adiabatic}}(T{=}T)$. The ΔG parameter is then evaluated as

$$\Delta G = \text{IP}_{\text{adiabatic}}(A) - \text{EA}_{\text{adiabatic}}(T{=}T) - \frac{14.4}{\varepsilon_{\text{static}} R} - E^*_{\text{adiabatic}} \quad (1)$$

where $\varepsilon_{\text{static}}$ is the solvent's static dielectric constant (ca. 78) and R is the distance between the donor A and acceptor T=T in Å.

5. The electronic excitation energy $E^*_{\text{adiabatic}}$ is obtained as the energy $E_{A^*}(A^*)$ of the photoexcited A* (equilibrated in water) at its equilibrium geometry minus the energy $E_A(A)$ of the ground-state A (equilibrated in water) at its own equilibrium geometry.

The reorganization energy λ, which characterizes the solvent's static minus optical dielectric response and the solutes' corresponding geometry relaxation, is the energy of the red dot in Figure 3 minus the energy of the blue dot, which is equal to $\Delta - \Delta G$. To obtain the energy change Δ associated with vertical (i.e., keeping geo-

dx.doi.org/10.1021/jp411666a | J. Phys. Chem. A 2014, 118, 7194−7200

metries frozen and allowing only for nonequilibrium solvent response) transfer of an electron from A* to T=T, we did the following.

6. We computed the energy $E_{A^+}(A^*)$ of the cation A^+ at the photoexcited neutral A*'s equilibrium geometry (determined in a dielectric environment having $\varepsilon = 78$) allowing only for the nonequilibrium (i.e., high-frequency) response of the solvent.
7. We computed the energy $E_{TT-}(TT)$ of anionic $T{=}T^-$ at the neutral T=T's equilibrium geometry (determined in a dielectric environment having $\varepsilon = 78$) allowing only for the nonequilibrium (i.e., high-frequency) response of the solvent.
8. $E_{A^+}(A^*) - E_{A^*}(A^*)$ is the vertical IP of the photoexcited A*, $IP_{vertical}(A^*)$.
9. $E_{TT}(TT) - E_{TT-}(TT)$ is the vertical EA of T=T, $EA_{vertical}(T{=}T)$.
10. $IP_{vertical}(A^*) - EA_{vertical}(T{=}T)$ is a quantity we define as δE and is the energy required to vertically remove an electron from the photoexcited donor and vertically place the electron onto the T=T acceptor but ignoring the Coulomb interaction between the donor cation and acceptor anion (which we treat separately).
11. In turn, δE plus the Coulomb interaction $-14.4/\varepsilon_\infty R$ between the A^+ cation and the $T{=}T^-$ anion (screened by the high-frequency dielectric constant ε_∞) gives Δ.

So, the reorganization energy, which is $\Delta - \Delta G$, can be expressed as

$$\lambda = \delta E - \Delta G - \frac{14.4}{\varepsilon_\infty R}$$
$$= IP_{vertical}(A^*) - IP_{adiabatic}(A) - EA_{vertical}(T{=}T) + EA_{adiabatic}(T{=}T) - \frac{14.4}{\varepsilon_\infty R} + \frac{14.4}{\varepsilon_{static} R} + E^*_{adiabatic} \quad (2)$$

Finally, once λ and ΔG are known, the activation energy can be estimated as

$$E^{act} = \frac{(\lambda + \Delta G)^2}{4\lambda} \quad (3)$$

The above prescription was also followed to estimate parameters arising when neutral O is the electron donor. However, when anionic A^- is the electron donor,

$$\Delta G = DE_{adiabatic}(A^-) - EA_{adiabatic}(T{=}T) - E^*_{adiabatic} \quad (4)$$

where $DE_{adiabatic}$ (A^-) is the adiabatic (i.e., with geometry relaxation and equilibrium solvent response) electron detachment energy of A^- and $E^*_{adiabatic}$ is the adiabatic electronic excitation energy of A^-. There is no Coulomb stabilization term in eq 4 because the electron-transfer process does not generate a cation−anion pair in this case, but eq 2 still is used to compute λ with anion detachment energies replacing neutral ionization potentials. This same prescription was used when O^- is the electron donor.

3. RESULTS

A. Vertical and Adiabatic Ionization Potentials, Detachment Energies, Electron Affinities, and donor $\pi\pi^*$ Excitation Energies. In Table 1, we display the adiabatic (i.e., with geometry relaxation and equilibrium solvent response) and vertical (i.e., with geometry frozen at the ground-state neutral geometry and with nonequilibrium solvent response) ionization potentials of 8-aminoguanine as well as this molecule's computed vertical and adiabatic singlet $\pi\pi^*$ excitation energies for $\varepsilon = 78$ computed as detailed in section 2. For comparison, the corresponding values for 8-oxoguanine are given below the data for A. Also, the energies δE, which are the vertical IPs (or DEs) of the photoexcited donor minus the vertical EA of the T=T donor are listed. Finally, the vertical and adiabatic electron affinities of the T=T electron acceptor are also shown. When the deprotonated species A^- or O^- are used as electron donors, the analogous energies given in Table 2 arise.

Table 1. Adiabatic and Vertical Ionization Potentials, Vertical and Adiabatic $\pi\pi^*$ Excitation Energies, and δE[a] Values of A and O; Adiabatic and Vertical EAs of T=T (All in eV)

A	$IP_{vertical}$	$IP_{adiabatic}$	δE	$E_{\pi\pi^*,vertical}$	$E^*_{adiabatic}$
$\varepsilon = 78$	6.9	5.3	2.5	4.5	4.1
O	$IP_{vertical}$	$IP_{adiabatic}$	δE	$E_{\pi\pi^*,vertical}$	$E^*_{adiabatic}$
$\varepsilon = 78$	7.1	5.6	2.8	4.4	4.3
T=T	$EA_{vertical}$	$EA_{adiabatic}$			
$\varepsilon = 78$	0.8	1.5			

[a] δE is Δ absent the Coulomb interaction term.

Table 2. Adiabatic and Vertical Detachment Energies, Vertical and Adiabatic $\pi\pi^*$ Excitation Energies, and δE[a] Values of A^- and O^-; Adiabatic and Vertical EAs of T=T (All in eV)

A^-	$DE_{vertical}$	$DE_{adiabatic}$	δE	$E_{\pi\pi^*,vertical}$	$E^*_{adiabatic}$
$\varepsilon = 78$	6.2	5.1	1.4	4.5	4.4
O	$DE_{vertical}$	$DE_{adiabatic}$	δE	$E_{\pi\pi^*,vertical}$	$E^*_{adiabatic}$
$\varepsilon = 78$	6.3	5.3	2.0	4.7	4.4
T=T	$EA_{vertical}$	$EA_{adiabatic}$			
$\varepsilon = 78$	0.8	1.5			

[a] δE is Δ absent the Coulomb interaction term.

B. Gibbs Free Energy Changes and Solvent Reorganization Energies. For the A molecule under study here, the data in Table 1 produce the following estimates of λ and ΔG from eqs 1 and 2:

$$\Delta G = 5.3 - 1.5 - 4.1 - \frac{14.4 \times 0.13}{R}$$
$$= -0.3 - \frac{0.2}{R}\ \text{eV} \quad (5)$$

$$\lambda = 2.5 + 0.3 - \frac{14.4}{R}\left(\frac{1}{1.8} - \frac{1}{78}\right)$$
$$= 2.8 - \frac{7.8}{R}\ \text{eV} \quad (6)$$

The corresponding values when O serves as the donor are

$$\Delta G = 5.6 - 1.5 - 4.3 - \frac{14.4 \times 0.13}{R}$$
$$= -0.2 - \frac{0.2}{R}\ \text{eV} \quad (7)$$

dx.doi.org/10.1021/jp411666a | J. Phys. Chem. A 2014, 118, 7194−7200

$$\lambda = 2.8 + 0.2 - \frac{14.4}{R}\left(\frac{1}{1.8} - \frac{1}{78}\right)$$
$$= 3.0 - \frac{7.8}{R}\ \text{eV} \quad (8)$$

When the data in Table 2 are used in eqs 2 and 4 to estimate λ and ΔG with A^- or O^- as the donor, we obtain $\lambda = 2.2 - 7.8/R$ eV; $\Delta G = -0.8$ eV for A^- and $\lambda = 2.6 - 7.8/R$ eV; $\Delta G = -0.6$ eV for O^-. These predictions are collected in Table 3.

Table 3. ΔG and λ Values (eV) for the Neutral and Anionic Donor Species Showing Dependence on the Donor−Acceptor Distance R (Å)

donor	ΔG	λ
A	$-0.3 - 0.2/R$	$2.8 - 7.8/R$
O	$-0.2 - 0.2/R$	$3.0 - 7.8/R$
A^-	−0.8	$2.2 - 7.8/R$
O^-	−0.6	$2.6 - 7.8/R$

There are four features that merit discussion when the data on these four potential electron donors are compared. First, the reorganization energy depends strongly on the separation between the donor and acceptor, whereas ΔG varies less strongly if at all. Second, the ΔG values differ among the four donors in two ways: (1) ΔG is more favorable (i.e., more negative) for the anion donors and (2) ΔG is more favorable for A than for O and for A^- than for O^-. Third, the λ values for the neutral donors are larger than for the anionic donors. Fourth, λ is smaller for A than for O and smaller for A^- than for O^-. As we illustrate below, these differences in λ and ΔG produce *differences* in the predicted activation barriers for A and O and for A^- and O^-. However, before showing the barrier heights that result from the above analysis, we want to offer two sets of data that suggest that the relative energies we use to predict these barriers are reasonable.

C. Comparison with Marcus' Method for Estimating Reorganization Energies. The reorganization energy λ can alternatively be expressed in terms of donor and acceptor radii, which, in turn, are given in terms of solvation free energies $\Delta G_{solvation}$ through

$$\Delta G_{solvation} = -\frac{14.4}{2R_{ion}}[\varepsilon_{static}^{-1} - 1] \quad (9)$$

Using radii determined from solvation data and eq 9, the reorganiztion energy is then expressed as[18]

$$\lambda = [\varepsilon_\infty^{-1} - \varepsilon_{static}^{-1}]\left\{\frac{14.4}{2R_{D^+}} + \frac{14.4}{2R_{T=T^-}} - \frac{14.4}{R}\right\} \quad (10)$$

We obtained solvation free energies of −2.68, −2.67, and −2.51 eV, respectively, for O^+, A^+, and $T{=}T^-$ from which we extracted radii from which we generated solvent reorganization energies of $2.85 - 7.8/R$ and $2.86 - 7.8/R$ eV for $A^+\cdots T{=}T^-$ and $O^+\cdots T{=}T$, respectively, which are within ca. 0.15 eV the λ values shown in Table 3. We view this comparison as suggesting there are no major flaws in our approach to estimating λ. In fact, the λ values obtained as we do using eq 2 are likely more accurate than those derived from the solvation free energies because the latter are based on spherical models of the donor and acceptor species within the Born solvation energy expression.

D. Comparison to TD-DFT Estimates of Charge-Transfer-State Energies. Before discussing how we use the ΔG and λ data to estimate the relative rates of barrier access for A, O, A^-, and O^-, it is instructive to compare how the energy of the charge-transfer-state E_{CT} predicted using donor IP and acceptor EA data compare to direct TD-DFT calculations of E_{CT}. This comparison is useful because it is much less computationally taxing to evaluate IP, EA, and $E^*_{adiabatic}$ and to then evaluate the donor cation to acceptor anion Coulomb interaction as $14.4/\varepsilon_\infty R$ than to carry out TD-DFT calculations of E_{CT} at several R values. If, as we now demonstrate to be the case, the former approach's predictions agree reasonably with the latter's, one can use the former with reasonable confidence.

To address this issue, we carried out a series of TD-DFT calculations of the vertical E_{CT} for an $O\cdots T{=}T$ complex at five values of the O-to-T=T separation and with the O and T=T aligned as they are in DNA oligomers like those shown in Figure 2. In this context, the term vertical means that the geometry is that of the neutral $O\cdots T{=}T$ and the solvent response is treated in a nonequilibrium manner as described in section 2. From Figure 3, we see that the vertical electronic excitation energy from the ground state to the charge-transfer state can be expressed in terms of vertical IP and vertical EA data (from Table 1) as follows

$$E_{CT} = IP_{vertical}(O) - EA_{vertical}(T{=}T) - \frac{14.4}{\varepsilon_\infty R} \quad (11)$$

In Table 4, we show how the values of E_{CT} determined from eq 11 compare to those calculated directly from nonequilibrium TD-DFT theory.

Table 4. Charge-Transfer Vertical Excitation Energies (eV) Computed from Eq 11 and from TD-DFT Theory at Five Values of the O-to-T=T Separation R (Å)

R (Å)	E_{CT} from eq 11	E_{CT} from TD-DFT
7	5.2	5.1
8	5.3	5.2
10	5.5	5.3
12	5.6	5.4
15	5.8	5.6

First, we notice that the E_{CT} values resulting from our TD-DFT calculations vary with R in a manner that very closely tracks the $14.4/\varepsilon_\infty R$ dependence with a value of ε_∞ near 1.8, as expected. We also notice that the E_{CT} values obtained from eq 11 are very close to, but systematically 0.1−0.2 eV above, those obtained from TD-DFT. This comparison of E_{CT} values computed in two independent manners, suggests that estimating values of E_{CT} using IP and EA data, combined with a $14.4/\varepsilon_\infty R$ R dependence, can be expected to be as reliable (±0.2 eV) as using TD-DFT methods. Therefore, for the remainder of this study, we will use IP, DE, EA, and $E^*_{adiabatic}$ data combined with analytical expressions for cation−anion Coulomb interactions to estimate free energies and, in the next section, electron-transfer barrier heights.

E. Charge-Transfer Activation Barriers. To estimate the activation energies for electron transfer using eq 3, we need to specify the donor−acceptor distance R. To examine the R dependence of the activation barriers, we will use R values of 4, 7, 10, and 15 Å. The first three values are in the ranges expected for first, second, and third neighbors within DNA oligomers such as shown in Figure 2. The R = 15 Å estimates are included

dx.doi.org/10.1021/jp411666a | J. Phys. Chem. A 2014, 118, 7194−7200

to illustrate that the activation barrier becomes too high at larger R because the Coulomb stabilization is too weak. In Table 5 we show values of ΔG, λ, and E^{act} for four values of the donor−acceptor distance R.

Table 5. ΔG, λ, and Charge-Transfer Activation Barriers (All in eV) for Four Values of the Donor−Acceptor Distance R (Å) and Four Potential Electron Donors[a]

donor →	neutral A	neutral O	anionic A^-	anionic O^-
$\Delta G(R=4)$	−0.35	−0.25	−0.8	−0.6
$\lambda(R=4)$	0.85	1.05	0.25	0.65
$E^{act}(R=4)$	**0.07**	**0.15**	**0.30**	**<0.01**
$\Delta G(R=7)$	−0.33	−0.23	−0.8	−0.6
$\lambda(R=7)$	1.69	1.89	1.09	1.49
$E^{act}(R=7)$	**0.27**	**0.36**	**0.02**	**0.13**
$\Delta G(R=10)$	−0.32	−0.22	−0.8	−0.6
$\lambda(R=10)$	2.02	2.22	1.42	1.82
$E^{act}(R=10)$	**0.36**	*0.45*	**0.07**	**0.20**
$\Delta G(R=15)$	−0.31	−0.21	−0.8	−0.6
$\lambda(R=15)$	2.28	2.48	1.68	2.02
$E^{act}(R=15)$	*0.43*	*0.52*	**0.12**	**0.26**

[a]In all cases, T=T is the electron acceptor.

In viewing these barrier heights, it is important to keep in mind that we are attempting to predict *differences* among A, O, A^-, and O^-, realizing that the absolute accuracy of the computed IP, DE, EA, and $E^*_{adiabatic}$ data limits the absolute accuracy of the computed barrier heights. Therefore, we also bring to bear the fact that we know from experimental data[3,4] as analyzed in refs 1 and 2 that photoexcited O is able to effect T=T repair at rates exceeding ca. 10^8 s^{-1} if the O-to-T=T distance is at or below ca. 7.5 Å (i.e., next-nearest neighbor distance in the DNA duplexes). This suggests that the barrier shown in bold for O at R = 7 Å (estimated to be 0.36 eV) can be thermally accessed and generate T=T repair rates in excess of 10^8 s^{-1}. However, assuming a solvent reorientation rate of 10^{12} s^{-1}, a barrier-access rate of 10^8 s^{-1} would require a barrier height of 0.23 eV or less. These realities suggest that our computed 0.36 eV barrier is too high by at least 0.1 eV. Moreover, the preceding section showed that donor−acceptor ion-pair energies calculated using IP, DE, EA, and $E^*_{adiabatic}$ data are probably 0.1−0.2 eV too high (e.g., the $E^*_{adiabatic}$ listed in Table 1 for O is 4.2 eV but we know that O absorbs 4.1 eV photons). Therefore, we think all the barriers listed in the table are overestimated by 0.1−0.2 eV, but we think the *relative barrier heights* among A, O, A^-, and O^- are more likely in the correct order. Hence, knowing that O effects T=T repairs at rates in excess of 10^8 s^{-1} at donor−acceptor distances out to ca. 7.5 Å, we show in bold in Table 5 all cases for which we expect barrier-access rates in excess of 10^8 s^{-1}. Those expected to produce rates significantly below 10^8 s^{-1} are italic.

To the extent that we can assume that the donor−acceptor electronic coupling strengths are, at any given R value, very similar for the four donors considered here, the data in Table 5 suggest the following:

1. A^- should be a somewhat better electron-transfer agent than O^- because A^- has a lower barrier than A^- at most donor−acceptor distances.
2. Neutral A should be better than neutral O at all donor−acceptor distances and might repair T=T out to R = 10 Å (third nearest neighbor) at rates similar to those of O at 7 Å (second nearest neighbor).
3. Anionic O^- and A^- should be better than neutral O or A at essentially all donor−acceptor distances.

The second prediction can be tested by using A in place of O within DNA duplexes analogous to those shown in Figure 2 allowing A to occupy nearest, second-nearest, and third-nearest neighbor positions relative to T=T.

Finally, we note that the predictions made above are based on the assumption that differences in barrier heights rather than in electronic coupling strengths govern differences in electron-transfer rates between A and O at any given R value. In support of this assumption, we offer the following analysis. We expect the rate of electron transfer from the photoexcited donor* to T-T to be proportional to $H_{a,b}{}^2 \exp(-E^{act}/RT)$, where $H_{a,b}$ is the electronic coupling matrix element between the donor*···T=T and donor$^+$···T=T$^-$ states. Within the generalized Mulliken−Hush theory,[19] this coupling is expressed as

$$H_{a,b} = \frac{\mu_{1,2}\Delta E_{1,2}}{\sqrt{\Delta\mu^2 + 4\mu_{1,2}{}^2}} \qquad (12)$$

where $\Delta E_{1,2}$ is the energy gap between the donor*···T=T and donor$^+$···T=T$^-$ states, $\mu_{1,2}$ is the transition dipole connecting these two states, and $\Delta\mu$ is the difference in the dipole moments of these state. We have the following information about these quantities for the donor···T=T pair that suggests that $H_{a,b}$ for A should be within ca. 10% of that for O.

(i) The $\pi\pi^*$ excitation energies and IPs of A and O are within 10% of one another, which, as we saw earlier, means that the values of $\Delta = \lambda + \Delta G$ and of λ are within 10% (Table 3). The energy gap $\Delta E_{1,2}$ appearing in eq 12 is (Figure 3) equal to Δ, so $\Delta E_{1,2}$ for A is within 10% of the value for O.

(ii) The dipole moment change $\Delta\mu$ accompanying the donor*···T=T to donor$^+$···T=T$^-$ transition is essentially identical for A and O because the π^*-orbital structures of these two donors are very similar. This dipole change can be approximated as eR, where e is the unit of charge and R is the distance between the donor and T=T defined earlier.

(iii) The transition dipole matrix element $\mu_{1,2}$ associated with the donor π^* to T=T π^* orbital transition should be very similar for A and O because (a) the oscillator strengths we obtained for the A and O $\pi\pi^*$ transitions are nearly identical (which suggests that the π and π^* orbitals of A and O are similar) and (b) the acceptor (T=T) is the same in both cases.

We note that $H_{a,b}{}^2$ appears linearly in the expression for the electron-transfer rate while the barrier height E^{act} appears within an exponential. The above discussion provides evidence that the ratio of $H_{a,b}{}^2$ values for A and O is within ca. 20% of unity. Therefore, it is the exponential dependence on E^{act}, with values of E^{act} that differ by ca. 0.1 eV from A to O and from A^- to O^- that largely determines the *relative* electron-transfer rates at any R value.

4. SUMMARY

Data from MP2- and DFT-level electronic structure calculations were used to estimate the *differences* in the barriers for $\pi\pi^*$ excited 8-aminoguanine compared to 8-oxoguanine (or the deprotonated anions of these donors) to transfer an electron to

dx.doi.org/10.1021/jp411666a | J. Phys. Chem. A 2014, 118, 7194−7200

proximal thymine dimer sites. Evidence is given to support the proposition that because A and O (and A^- and O^-) have very similar chemical compositions and bonding, geometries, and π-orbital characters, the electron-transfer rate *differences* among these four donors derive primarily from differences in electron-transfer barrier heights rather than from differences in donor−acceptor electronic coupling strengths at a given donor−acceptor separation.

The singlet $\pi\pi^*$ excitation energies $E^*_{\text{adiabatic}}$ and vertical and adiabatic ionization potentials (IP) (detachment energies (DE) for the deprotonated species) computed under conditions of both static and high-frequency solvent dielectric response were the primary data produced in our calculations. These data were used to estimate free energy ΔG, reorganization energy λ, and activation energy E^{act} parameters appropriate to electron transfer from photoexcited $\pi\pi^*$ states of the O, A, O^-, and A^- donors to the lowest-energy π^* orbital of a thymine dimer. The reliability of expressing these free energy values in terms of donor IP (or DE) and T=T EA values and dielectrically screened donor cation-T=T^--anion Coulomb interactions was tested by comparing energies of the ion-pair state thus estimated with independently computed TD-DFT charge-transfer-state energies for $O^+\cdots T{=}T^-$ at five donor−acceptor distances. The favorable outcome of this comparison means that the search for even better T=T repair agents can focus on finding molecules with lower vertical and adiabatic IPs than A but with π-orbital character similar to that of A (so as to retain A's $H_{a,b}{}^2$ strength) and with a singlet $\pi\pi^*$ absorption near the value of $E^*_{\text{adiabatic}}$ obtained here for A and O.

The Marcus activation barriers computed here suggest that 8-aminoguanine and its deprotonated derivative should be even better candidates as thymine dimer repair agents than 8-oxoguanine and its deprotonated derivative. The primary source of the lower activation barrier in A vs O (and A^- vs O^-) is the fact that A has a lower IP than O (and A^- has a lower DE than O^-). All four potential donors are predicted to have singlet $\pi\pi^*$ absorptions in approximately the same region and at energies below where DNA bases absorb and to have lower IPs (or DEs) than any of DNA bases. This means that they can be photoexcited without exciting any DNA base and that electron transfer will occur from them rather than from any DNA base. Specific predictions based on our estimates of barrier height *differences* have been put forth; hopefully, experiments will soon be carried out to test these predictions.

AUTHOR INFORMATION

Corresponding Author

*J. Simons: e-mail, simons@chem.utah.edu.

Notes

The authors declare no competing financial interest.

ACKNOWLEDGMENTS

We thank the Utah Center for High Performance Computing for resources and continued support, Professors Cynthia Burrows, Robert Cave, Pavel Jungwirth, and our reviewers for helpful suggestions, and Dr. Giovanni Scalmani for much technical assistance. We also acknowledge the Polish Ministry of Science and Higher Education grant No. 530-8371-D191-13 to P.S.

REFERENCES

(1) Anusiewicz, I.; Świerszcz, I.; Skurski, P.; Simons, J. Mechanism for Repair of Thymine Dimers by Photoexcitation of Proximal 8-oxo-7,8-dihydroguanine (OG). *J. Phys. Chem. A* **2013**, *117*, 1240−1253.

(2) Marchaj, M.; Sieradzan, I.; Anusiewicz, I.; Skurski, P.; Simons, J. Thymine dimer repair by electron transfer from photo-excited 2′,3′,5′-tri-O-acetyl-8-oxo-7,8-dihydroguanosine or 2′,3′,5′-tri-O-acetyl-ribosyluric acid- a theoretical study. *Mol. Phys.* **2013**, *111*, 1580−1588.

(3) Nguyen, K. V.; Burrows, C. J. A Prebiotic Role for 8-Oxoguanosine as a Flavin Mimic in Pyrimidine Dimer Photorepair. *J. Am. Chem. Soc.* **2011**, *133*, 14586−14589.

(4) Nguyen, K. V.; Burrows, C. J. Photorepair of cyclobutane pyrimidine dimers by 8-oxopurine nucleosides. *J. Phys. Org. Chem.* **2012**, *25*, 574−577.

(5) See, for example: Marcus, R. A. Chemical and Electrochemical Electron Transfer Theory. *Annu. Rev. Phys. Chem.* **1964**, *15*, 155. Newton, M. D. Quantum chemical probes of electron-transfer kinetics; the nature of donor-acceptor interactions. *Chem. Rev.* **1994**, *91*, 767−792.

(6) McLean, A. D.; Chandler, G. S. Contracted Gaussian basis sets for molecular calculations. I. Second row atoms, Z=11−18. *J. Chem. Phys.* **1980**, *72*, 5639−5648.

(7) Krishnan, R.; Binkley, J .S.; Seeger, R.; Pople, J. A. Self-consistent molecular orbitals methods. XX. A basis set for correlated wave functions. *J. Chem. Phys.* **1980**, *72*, 650−654.

(8) Lee, C.; Yang, W.; Parr, R. G. Development of the Colle-Salvetti correlation-energy formula into a functional of the electron density. *Phys. Rev. B* **1988**, *37*, 785−789.

(9) Becke, A. D. Density-functional exchange-energy approximation with correct asymptotic behavior. *Phys. Rev. A* **1988**, *38*, 3098−3100.

(10) Miertus, S.; Scrocco, E.; Tomasi, J. Electrostatic interaction of a solute with a continuum. A direct utilizaion of AB initio molecular potentials for the prevision of solvent effects. *Chem. Phys.* **1992**, *55*, 117−129.

(11) Miertus, S.; Tomasi, J. Approximate evalutations of the electronic free energy and internal energy changes in solution processes. *Chem. Phys.* **1982**, *65*, 239−245.

(12) Cossi, M.; Barone, V.; Cammi, R.; Tomasi, J. Ab initio study of solvated molecules: a new implementation of the polarizable continuum model. *Chem. Phys. Lett.* **1996**, *255*, 327−335.

(13) Bauernschmitt, R.; Ahlrichs, R. Treatment of electronic excitations within the adiabatic approximation of time dependent density functional theory. *Chem. Phys. Lett.* **1996**, *256*, 454−64.

(14) Casida, M. E.; Jamorski, C.; Casida, K. C.; Salahub, D. R. Molecular excitation energies to high-lying bound states from time-dependent density functional response theory: Characterization and correction of the time dependent local density approximation ionization threshold. *J. Chem. Phys.* **1998**, *108*, 4439−49.

(15) Scalmani, G.; Frisch, M. J.; Mennucci, B.; Tomasi, J.; Cammi, R.; Barone, V. J. Geometries and properties of excited states in the gas phase and in solution: Theory and application of a time-dependent density functional theory polarizable continuum model. *Chem. Phys.* **2006**, *124* (094107), 1−15.

(16) Yanai, T.; Tew, D.; Handy, N. A new hybrid exchange-correlation functional using the Coulomb-attenuating method (CAM-B3LYP). *Chem. Phys. Lett.* **2004**, *393*, 51−57.

(17) Frisch, M. J., Trucks, G. W., Schlegel, H. B., Scuseria, G. E., Robb, M. A., Cheeseman, J. R., Scalmani, G., Barone, V., Mennucci, B., Petersson; et al. *Gaussian 09*, Revision B.01; Gaussian, Inc.: Wallingford, CT, 2009.

(18) Marcus, R. A. On the Theory of Oxidation-Reduction Reactions Involving Electron Transfer I. *J. Chem. Phys.* **1956**, *24*, 966−978.

(19) Cave, R. J.; Newton, M. D. Calculation of electronic coupling matrix elements for ground and excited state electron transfer reactions: Comparison of the generalized Mulliken-Hush and block diagonalization methods. *J. Chem. Phys.* **1997**, *106*, 9213−9226.